Supporting Information

for

Reductive nitrosylation of nickel(II) complex by nitric oxide followed by release of nitrous oxide

Somnath Ghosh[a], Hemanta Deka[a], Yuvraj B. Dangat[b], Soumen Saha[a], Kuldeep Gogoi[a], Kumar Vanka[b] and Biplab Mondal[a,*]

[a]*Department of Chemsitry, Indian Institute of Technology Guwahati, Assam 781039, India*

[b]*Academy of Scientific and Innovative Research, National Chemical Laboratory, Pune 411008, Maharashtra, India*

Table of Contents

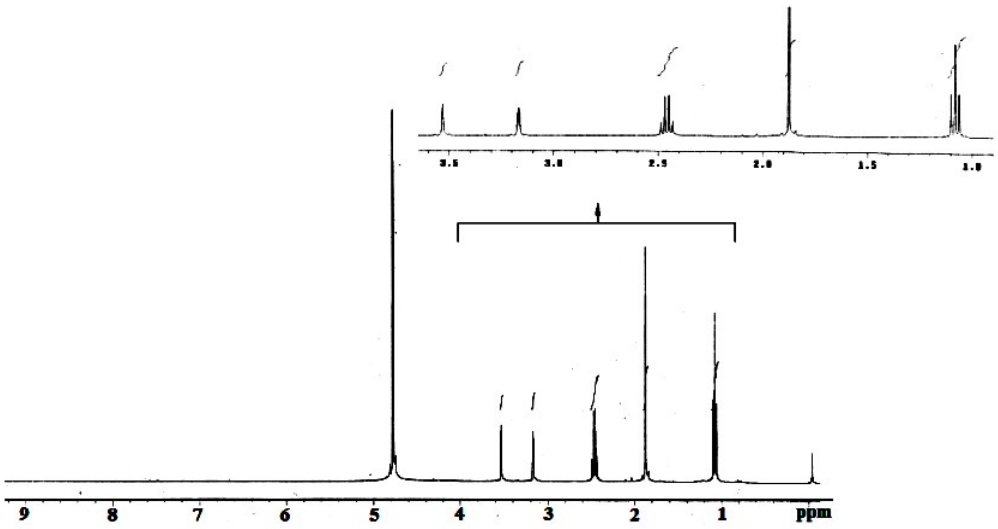

Figure S1: ^{1}H-NMR spectrum of **L** in methanol-d_4.

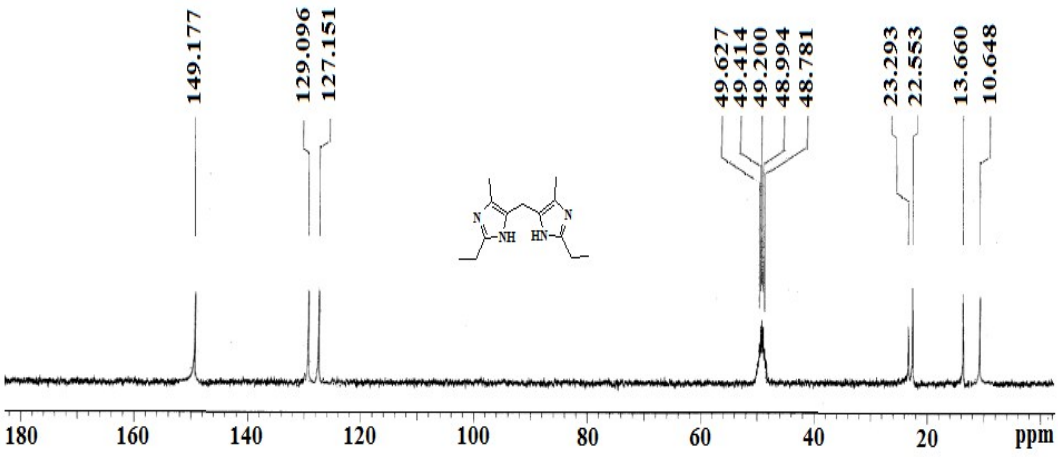

Figure S2: ^{13}C NMR spectrum of **L** in methanol-d_4.

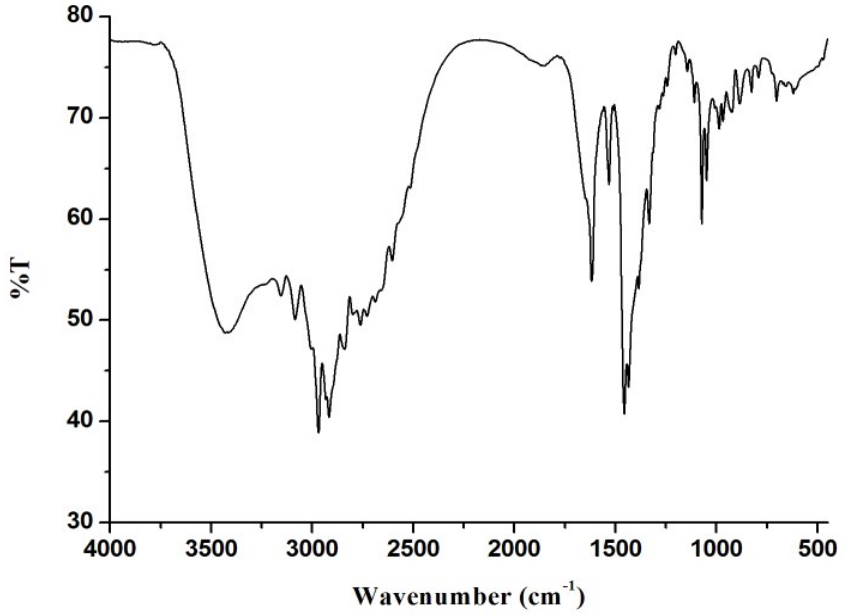

Figure S3: FT-IR spectrum of **L** in KBr.

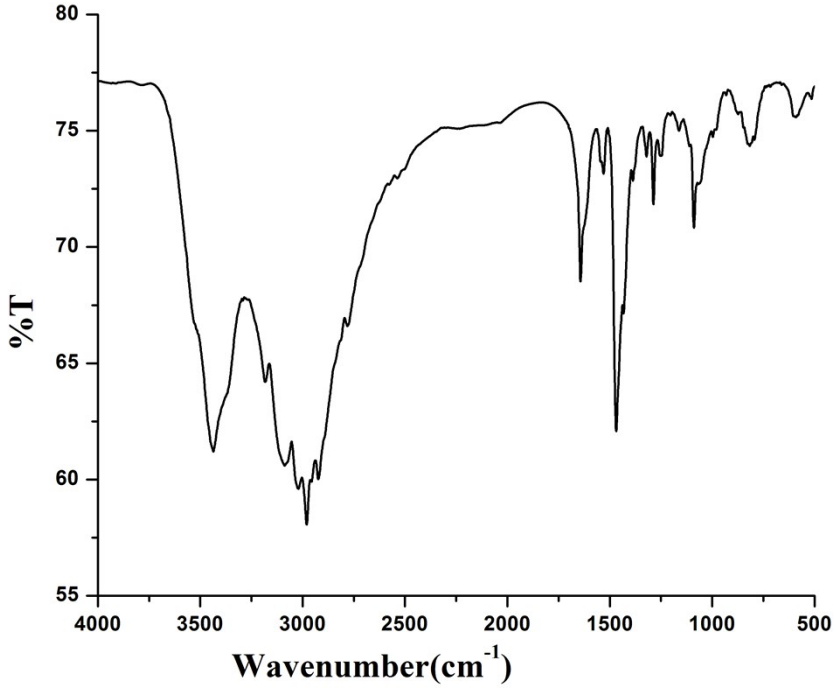

Figure S4: FT-IR spectrum of complex **1** in KBr.

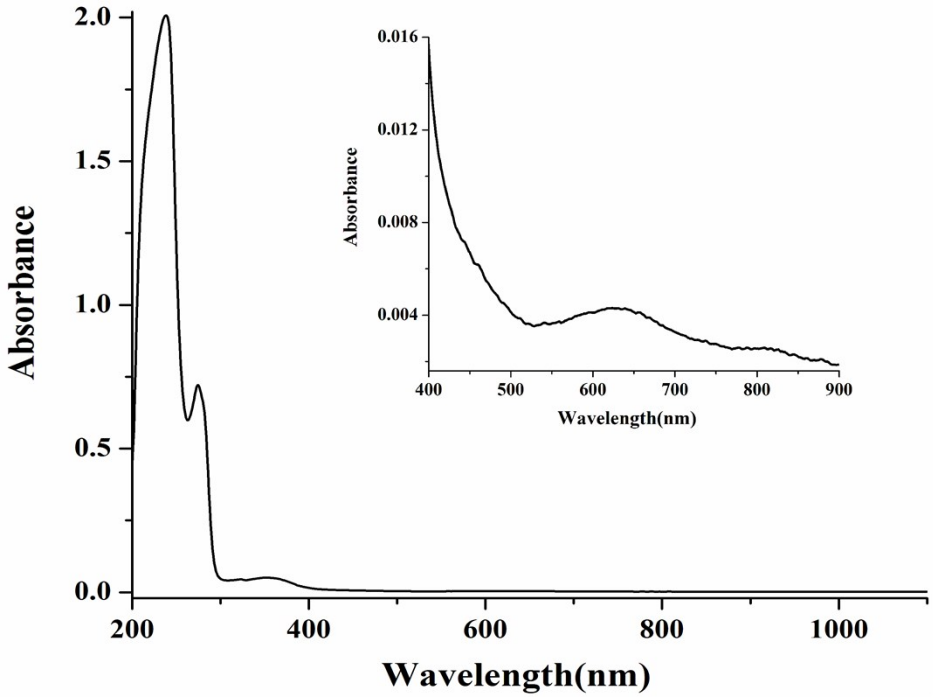

Figure S5: UV-visible Spectrum of complex **1** in dry methanol. Extinction coefficient at λ_{max} 636 nm is 25 lit.mol^{-1}.cm^{-1}.

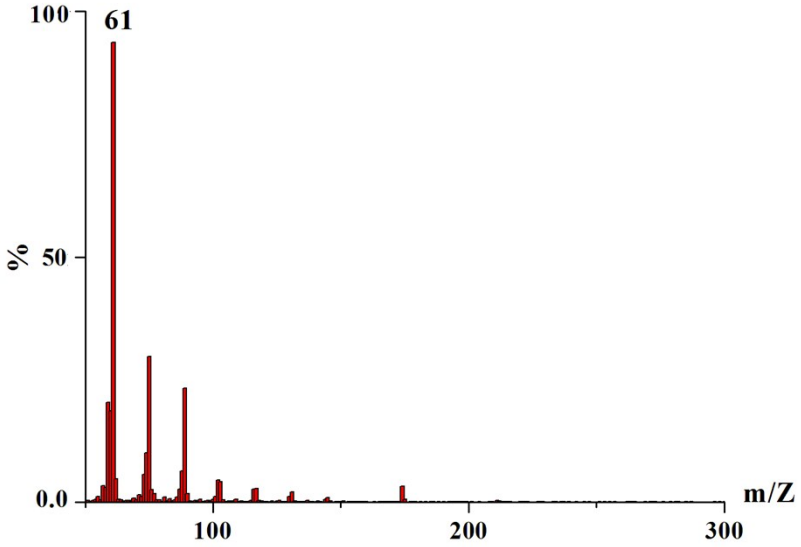

Figure S6: GC-mass spectra of methyl nitrite.

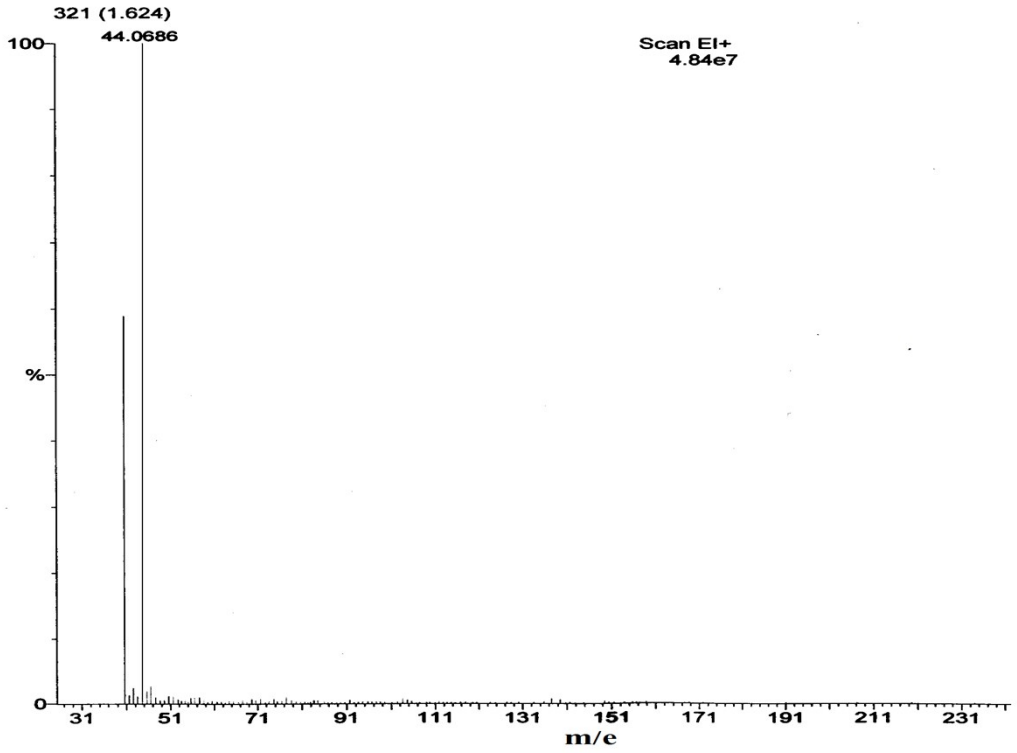

Figure S7: GC Mass spectra of N_2O, gas taken from the head space of the reaction mixture.

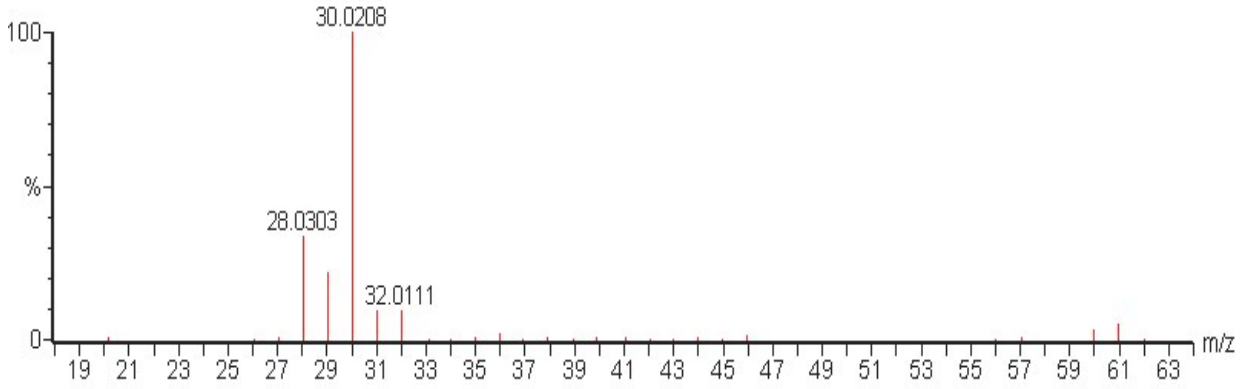

Figure S8: GC- Mass spectra of the head space gas taken from the round bottom flask containing dry MeOH and $NO_{(g)}$ purged into it (This suggests that N_2O does not form in the absence of the metal complex).

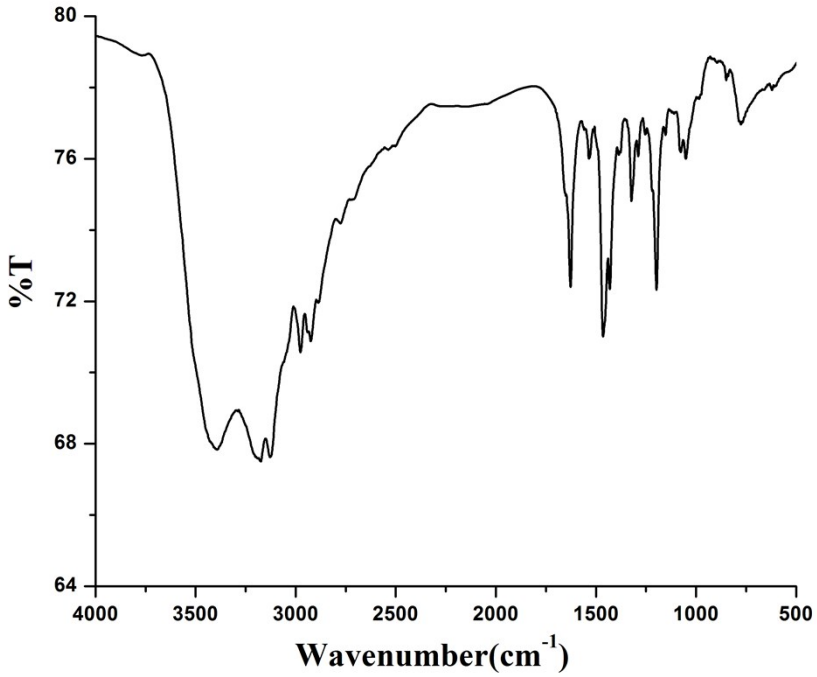

Figure S9: FT-IR spectrum of complex **2** in KBr.

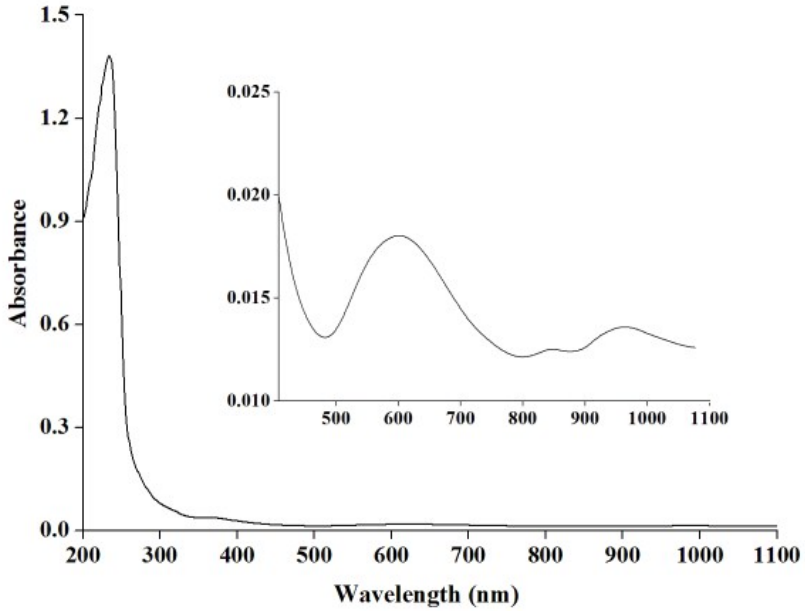

Figure S10: UV-visible Spectrum of complex **2** in dry methanol.

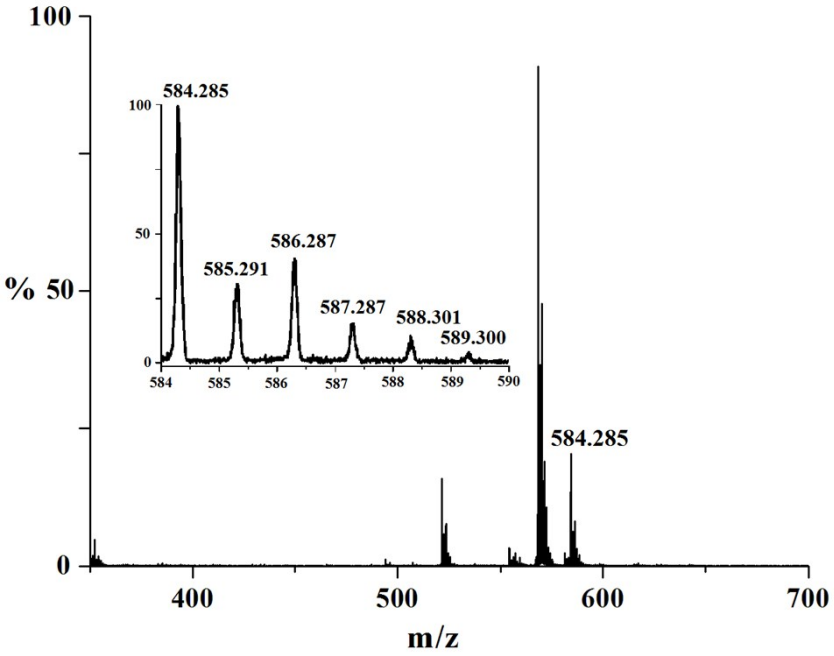

Figure S11: ESI Mass spectra of $[L_2Ni(NO)(CH_3OH)]^+$ in methanol (isotropic distribution pattern is shown inset).

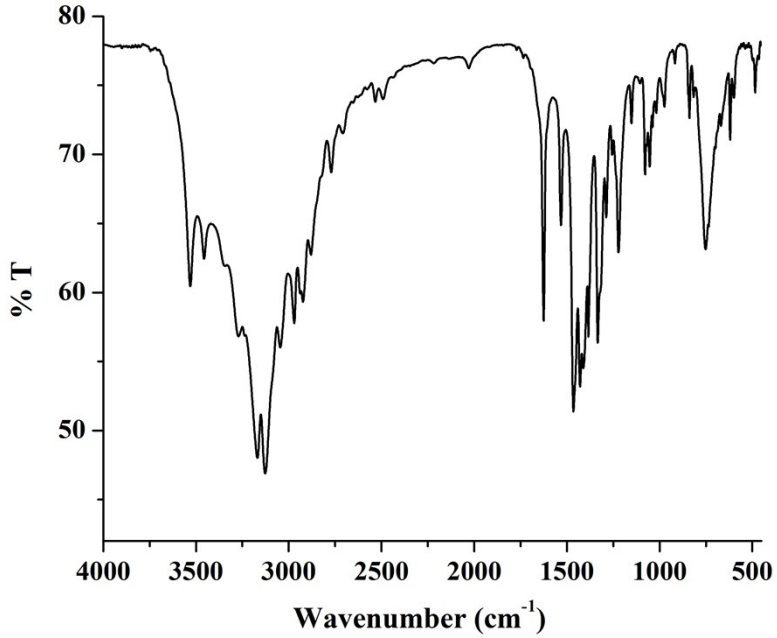

Figure S12: FT-IR spectrum of complex **3** in KBr.

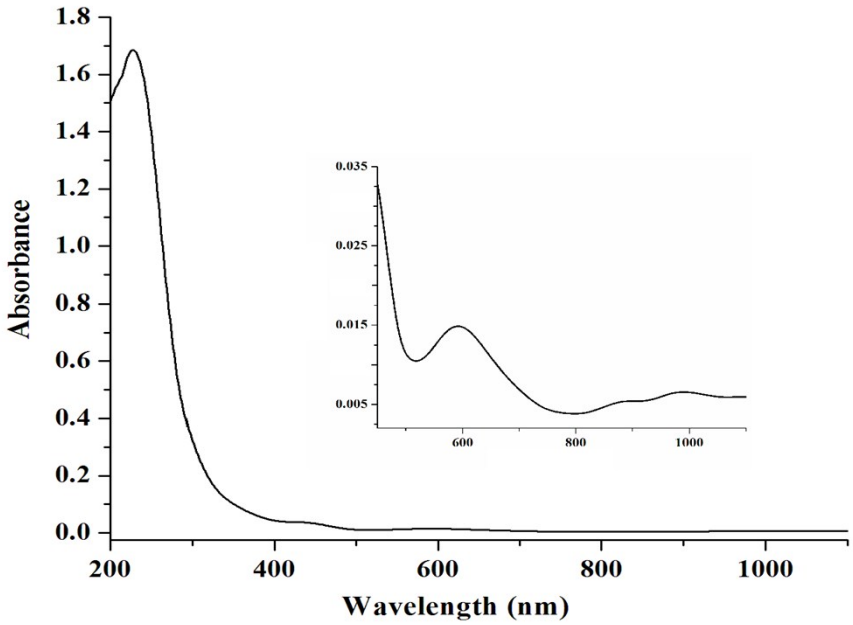

Figure S13: UV-Visible Spectrum of complex **3** in dry methanol.

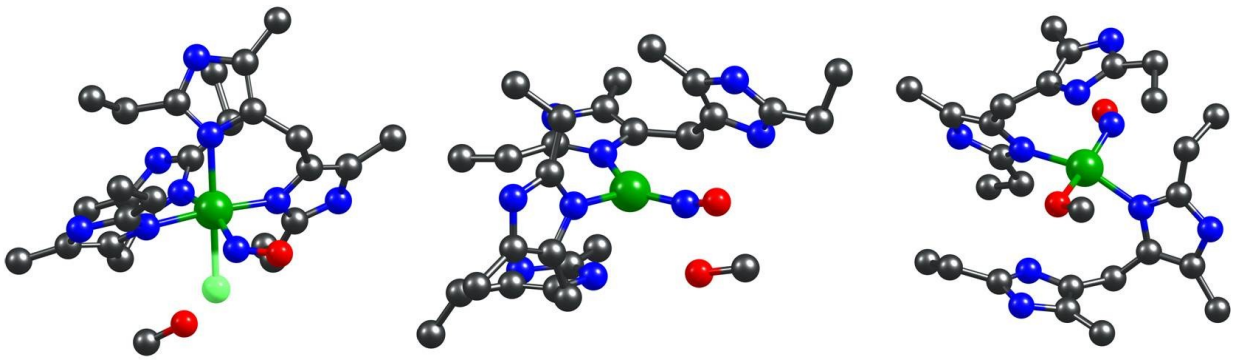

Figure S14: The possible structures corresponding to the proposed intermediate; the color scheme is as follows: nickel: green, chlorine: light green, carbon: black, oxygen: red, nitrogen: blue and hydrogen: white; the hydrogens have been removed for the purpose of clarity.

Cartesian coordinates for DFT optimized structure

C	-1.827	13.900	4.460	C	-1.552	11.407	0.081	H	0.346	7.981	0.944
C	-2.206	12.606	4.180	C	1.236	10.468	-2.105	H	1.790	8.652	0.163
N	-1.310	12.035	3.286	C	0.952	8.898	0.830	H	3.919	8.816	0.922
C	-0.390	12.963	3.013	C	1.479	9.329	2.166	H	4.641	8.377	2.488
N	-0.680	14.099	3.711	N	0.609	9.754	3.162	H	4.726	10.059	1.910
C	-3.343	11.808	4.738	C	1.356	10.151	4.191	H	1.335	11.748	5.588
C	-2.848	10.537	5.349	N	2.674	9.969	3.885	H	-0.195	10.887	5.394
N	-2.142	9.630	4.575	C	2.780	9.457	2.601	H	0.785	8.893	6.628
C	-1.820	8.600	5.359	C	-2.783	12.190	0.375	H	0.857	10.372	7.620
N	-2.303	8.834	6.612	C	-2.567	13.711	0.365	H	2.325	9.769	6.813
C	-2.958	10.055	6.634	C	0.887	10.745	5.476	H	-4.428	9.947	8.202
Ni	-1.455	9.999	2.697	C	1.236	9.892	6.706	H	-4.049	11.588	7.625
N	-2.367	8.556	2.150	C	4.085	9.163	1.951	H	-2.900	10.727	8.678
O	-2.245	7.988	1.087	O	-4.808	7.733	3.269	H	-4.060	11.563	3.931
C	-3.616	10.604	7.850	C	-5.158	8.202	4.574	H	-3.887	12.402	5.486
C	-1.089	7.366	4.959	H	-1.844	14.005	1.139	H	-3.297	14.546	5.858
C	0.775	12.863	2.089	H	-3.517	14.228	0.564	H	-2.708	15.839	4.785
C	2.077	13.405	2.696	H	-2.191	14.055	-0.610	H	-1.685	15.259	6.123
C	-2.406	14.942	5.351	H	-3.130	11.856	1.363	H	0.895	11.812	1.813
N	-0.998	10.481	0.863	H	-3.563	11.923	-0.358	H	0.546	13.411	1.157
C	0.105	9.961	0.199	H	0.765	10.161	-3.052	H	1.997	14.473	2.952
C	0.236	10.601	-1.012	H	1.982	9.708	-1.835	H	2.902	13.294	1.978
N	-0.818	11.501	-1.061	H	1.766	11.418	-2.284	H	2.340	12.851	3.610

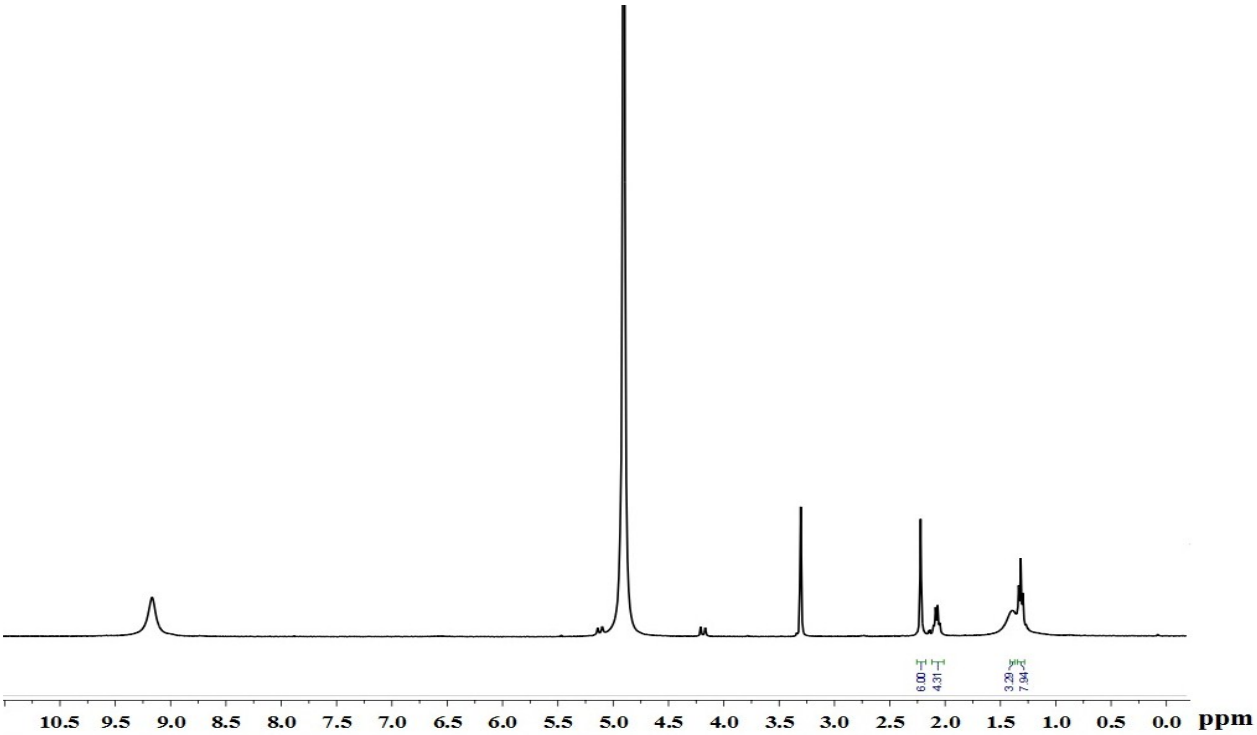

Figure S15: ^{1}H NMR spectrum of complex **1** in CD_3OD.

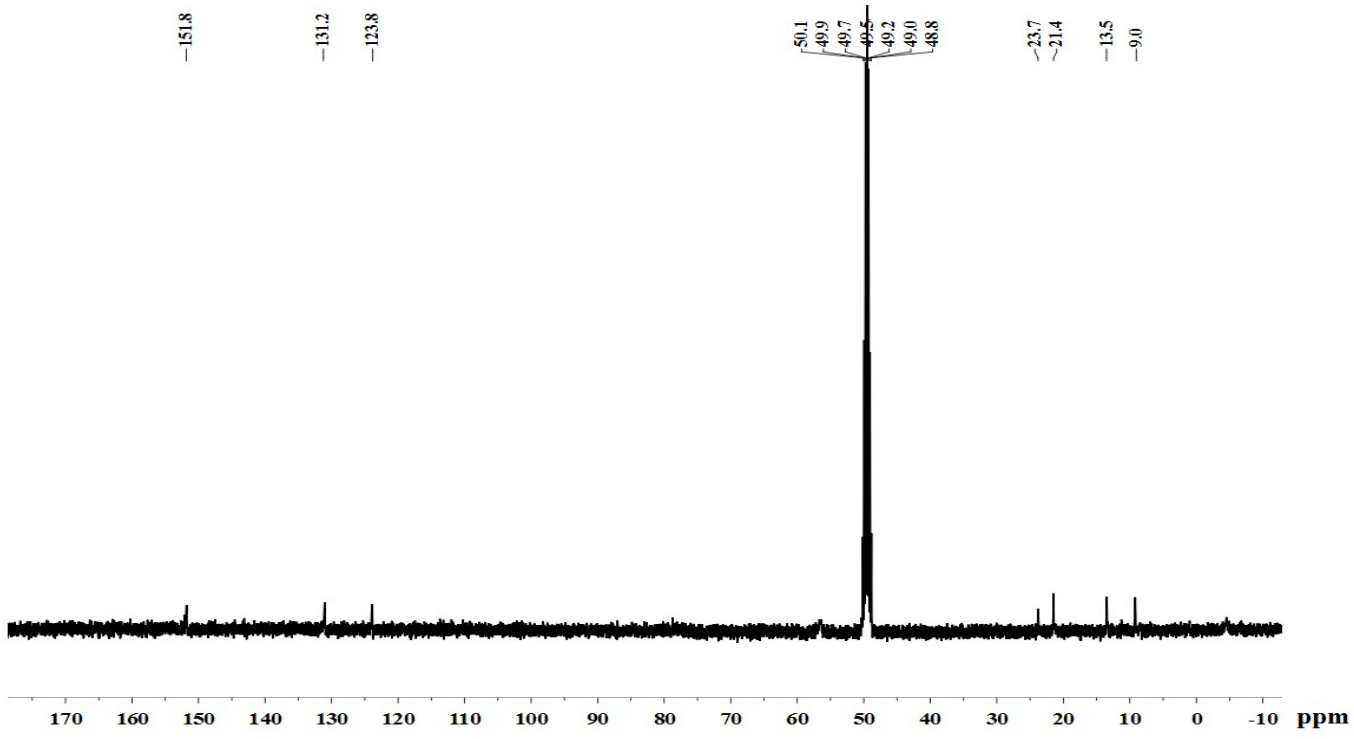

Figure S16: ^{13}C-NMR spectrum of complex **1** in CD_3OD.

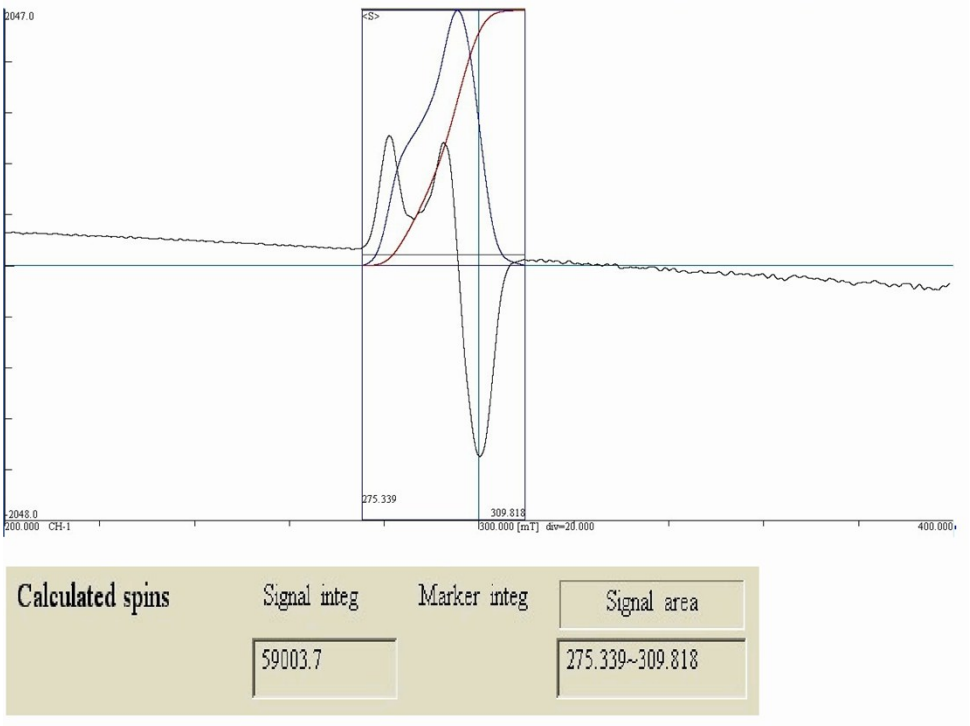

Figure S17: Double integration of EPR spectrum of Ni(I) species (concentration, 0.7 mmol) in methanol at 77K.

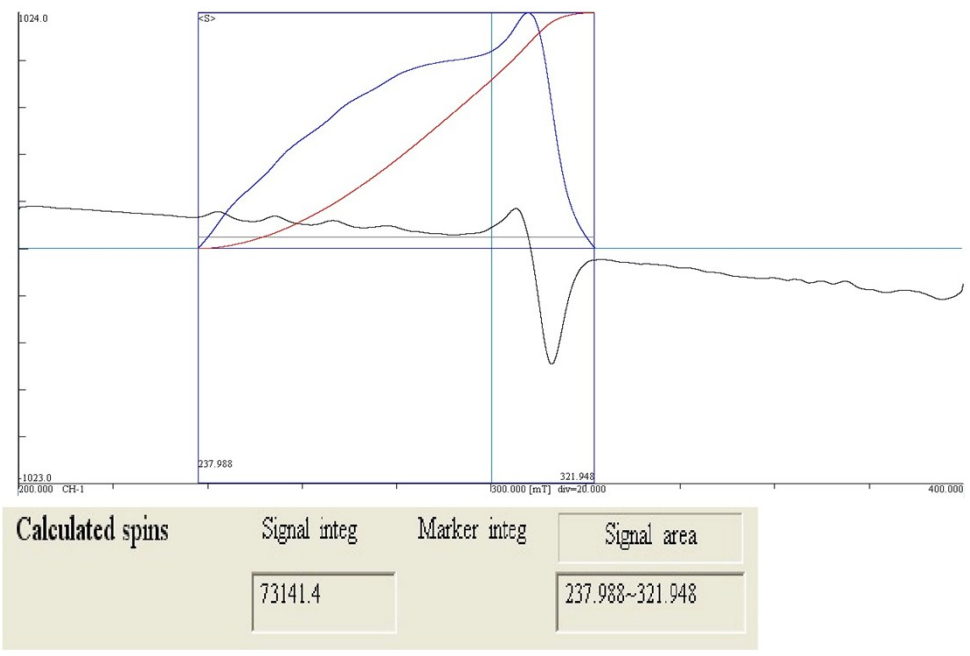

Figure S18: Double integration of standard $CuSO_4.5H_2O$ (concentration, 0.7 mmol) solution in methanol at 77K.

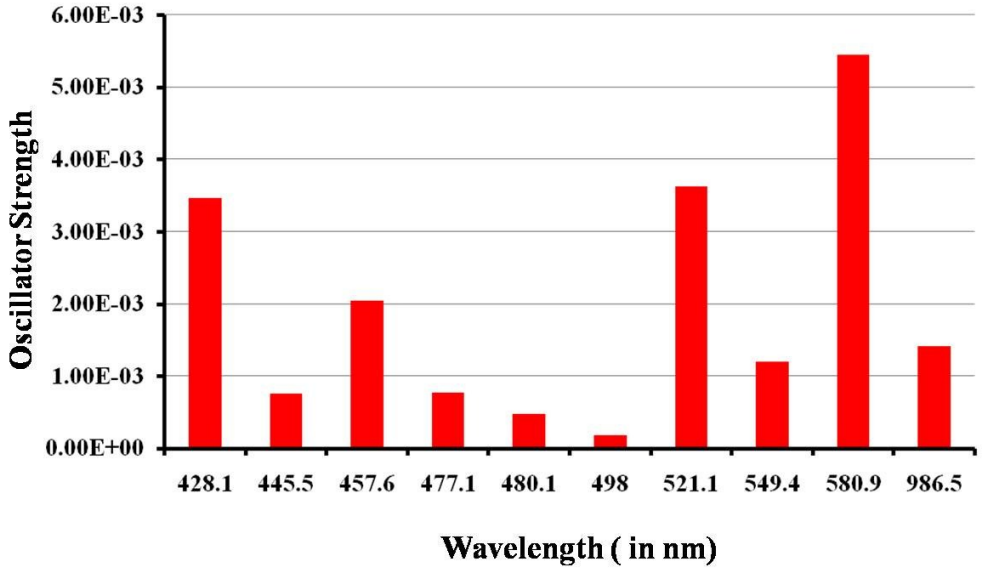

Figure S19: Plot of Oscillator strength *vs* Wavelength for intermediate $\{NiNO\}^{10}$ complex in methanol (ten excitations has been considered) using TD-DFT calculations at PBE/TZVP level of theory.

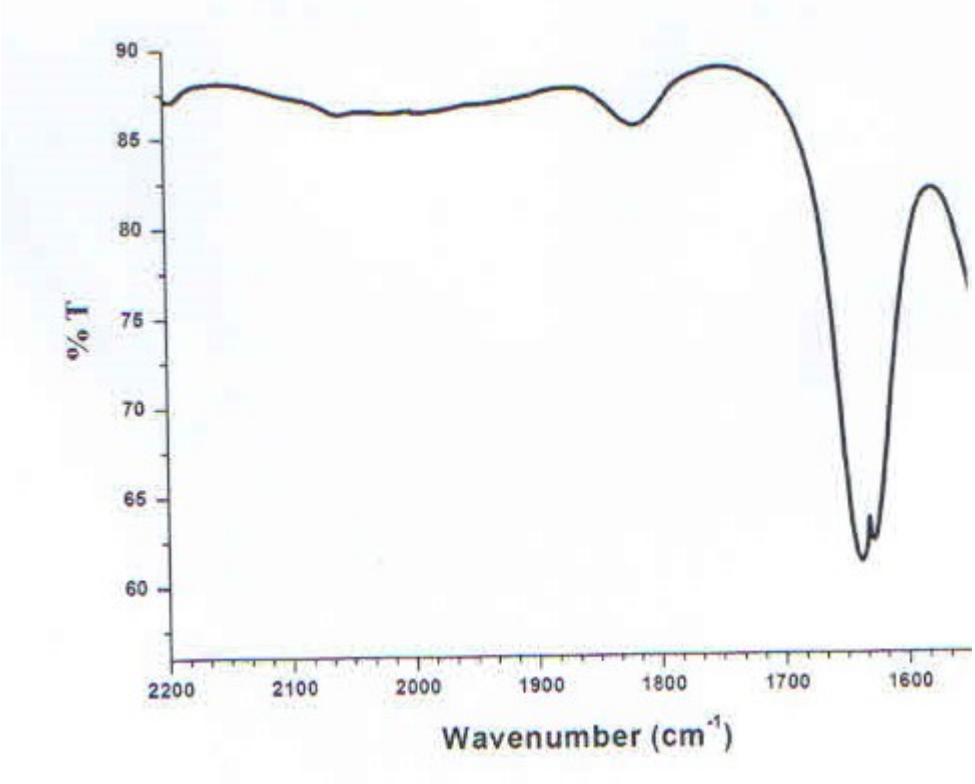

Figure S20: Solution FT-IR spectrum of $[L_2Ni(NO)(CH_3OH)]^+$ in methanol (with ^{15}NO; only 2200 – 1600 cm^{-1} range is shown for clarity).

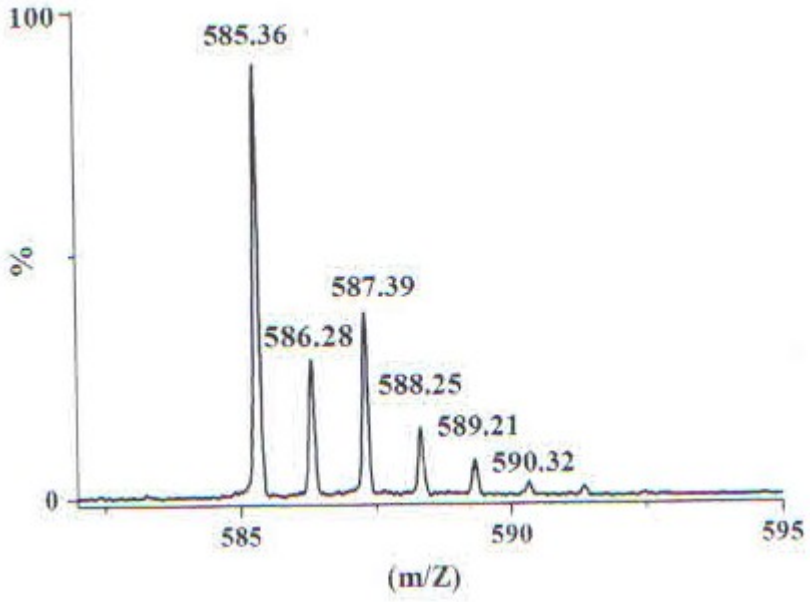

Figure S21: ESI Mass spectrum of $[L_2Ni(NO)(CH_3OH)]^+$ in methanol (with ^{15}NO)

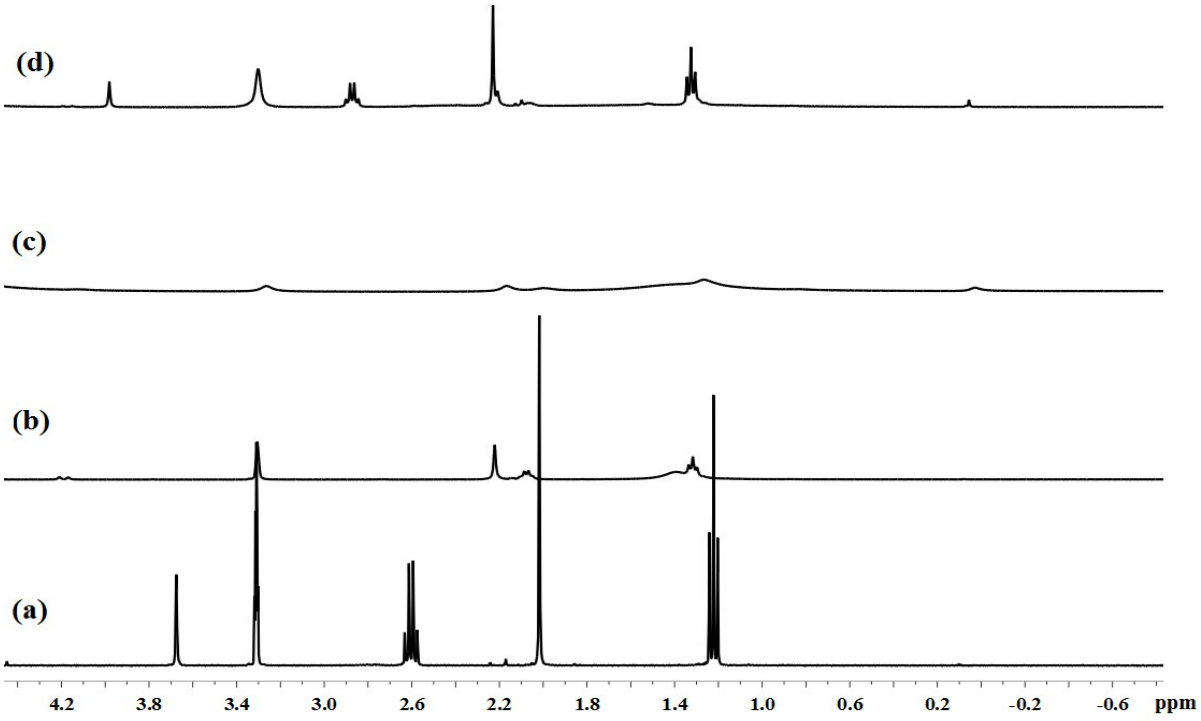

Figure S22: ^{1}H-NMR spectra of ligand, complex **1**, after purging 1 eq. of NO in complex **1** and after purging 2 eq. of NO in complex **1** are respectively **(a), (b), (c)** and **(d)** in CD_3OD.

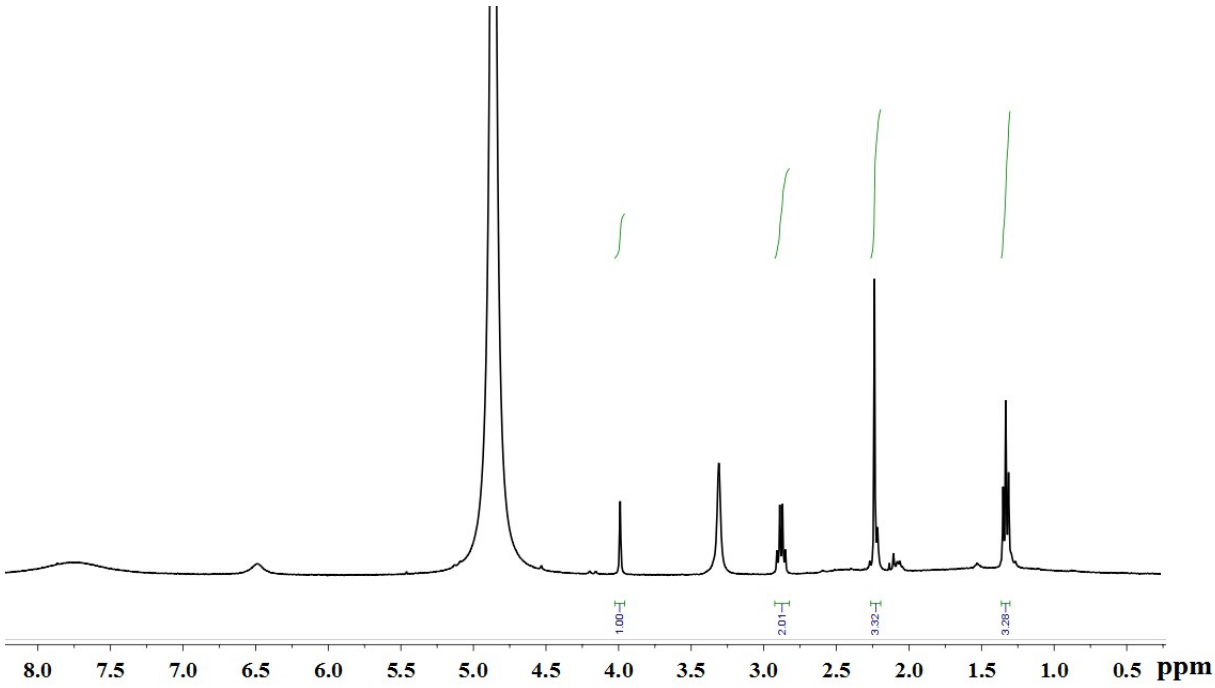

Figure S23: ^{1}H-NMR spectrum of complex **1** after purging 2 eq. of NO, in CD_3OD.

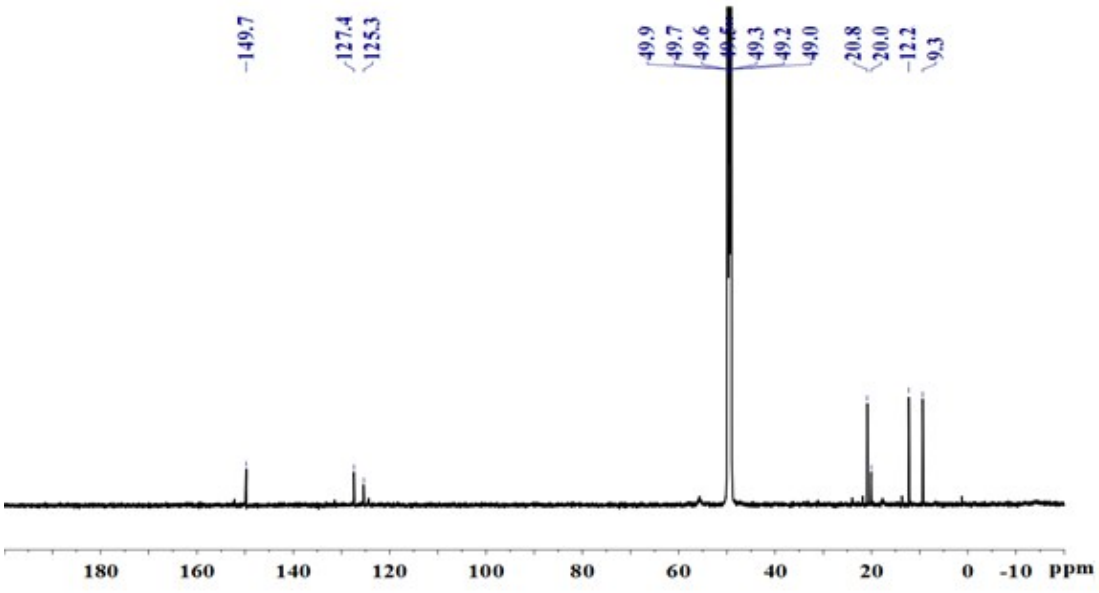

Figure S24: ^{13}C-NMR spectrum of complex **1** after purging 2 eq. of NO, in CD_3OD.

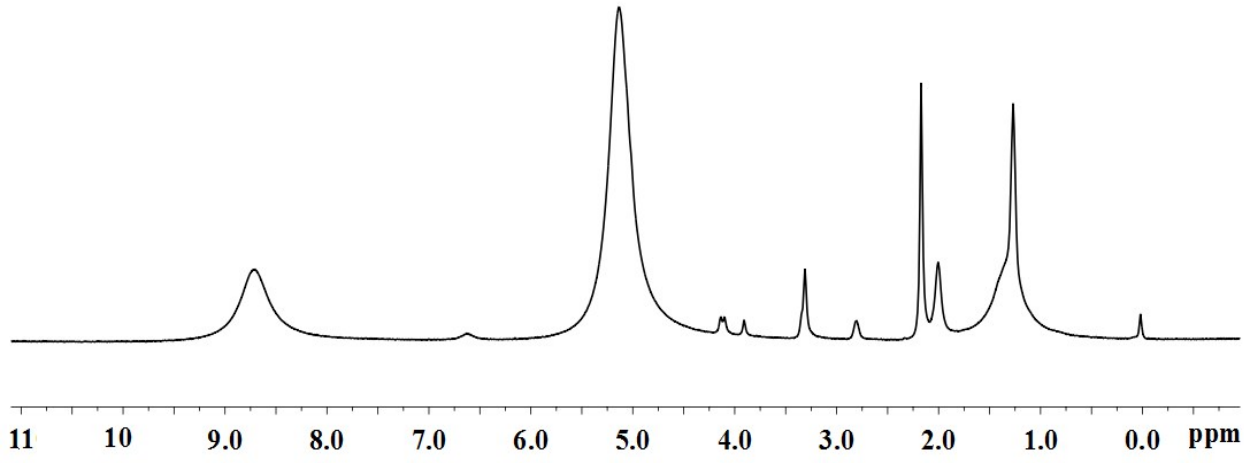

Figure S25: ^{1}H-NMR spectra of complex **2** in CD_3OD.

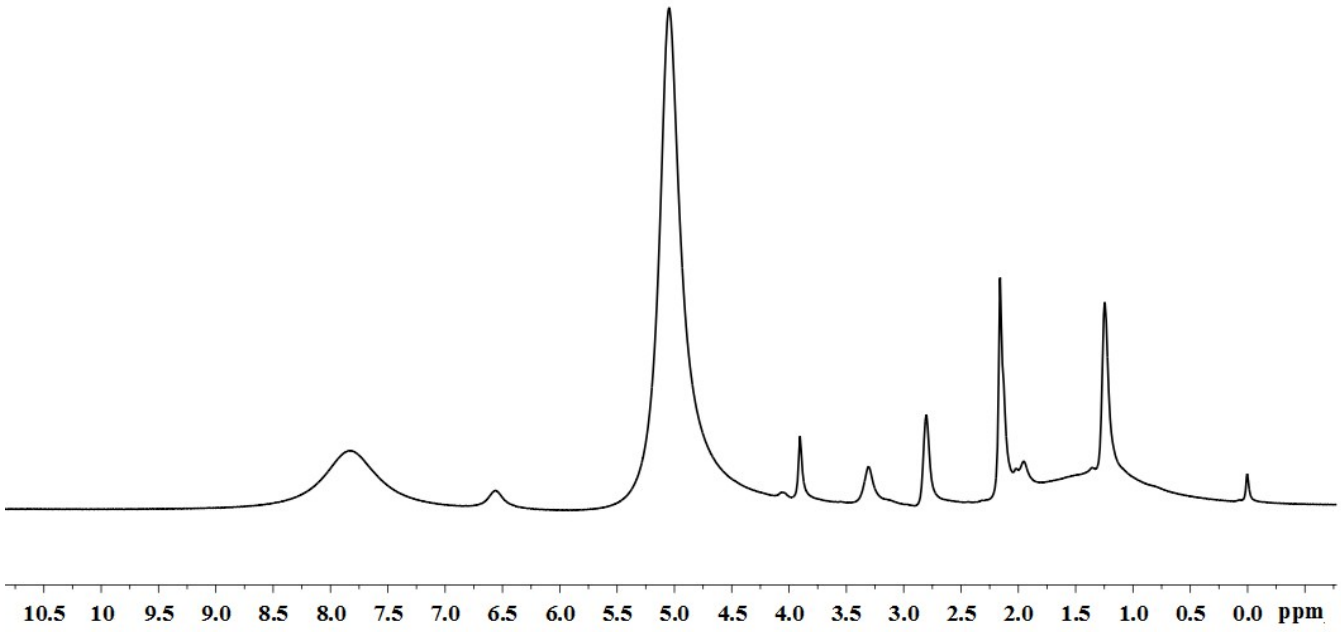

Figure S26: ^{1}H-NMR spectra of complex **3** in CD_3OD.

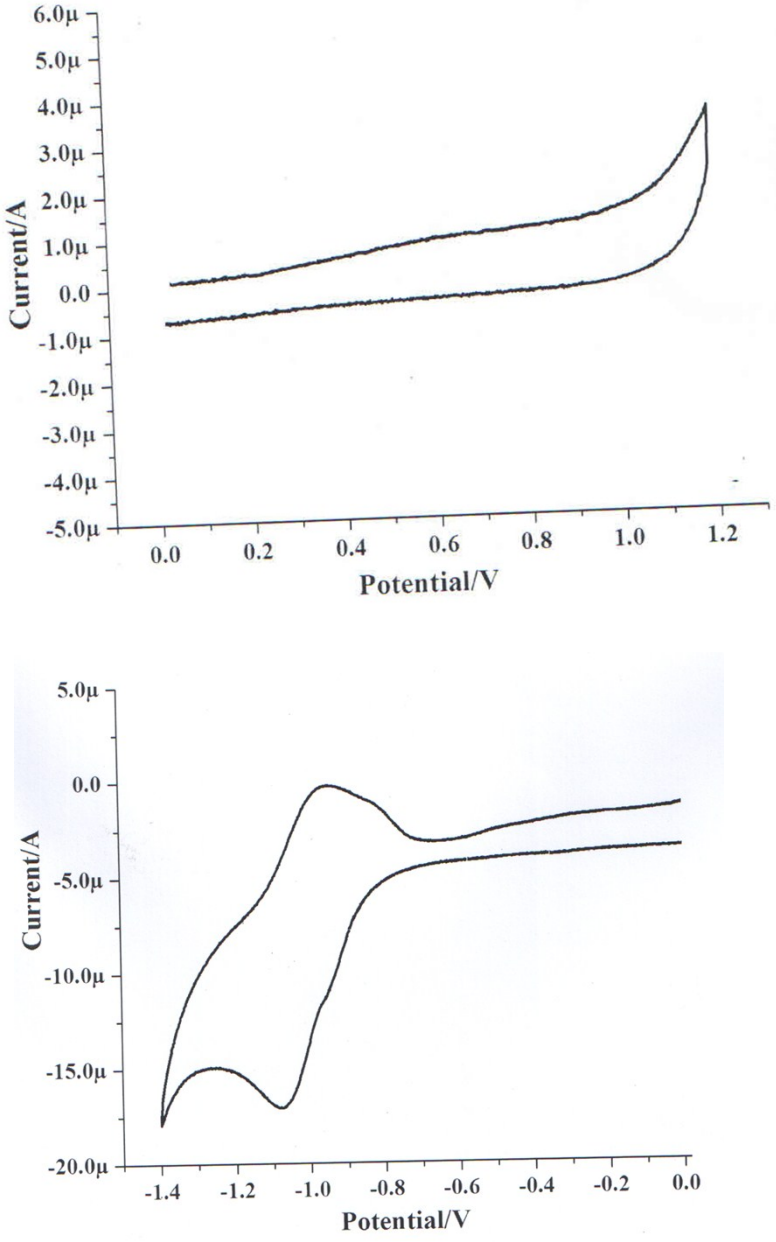

Figure S27: Cyclic voltammogram of complex **1** in methanol solvent. Working electrode, Glassy-carbon; Reference electrode, Ag/AgCl; TBAP supporting electrolyte; scan rate 50 mV/s.

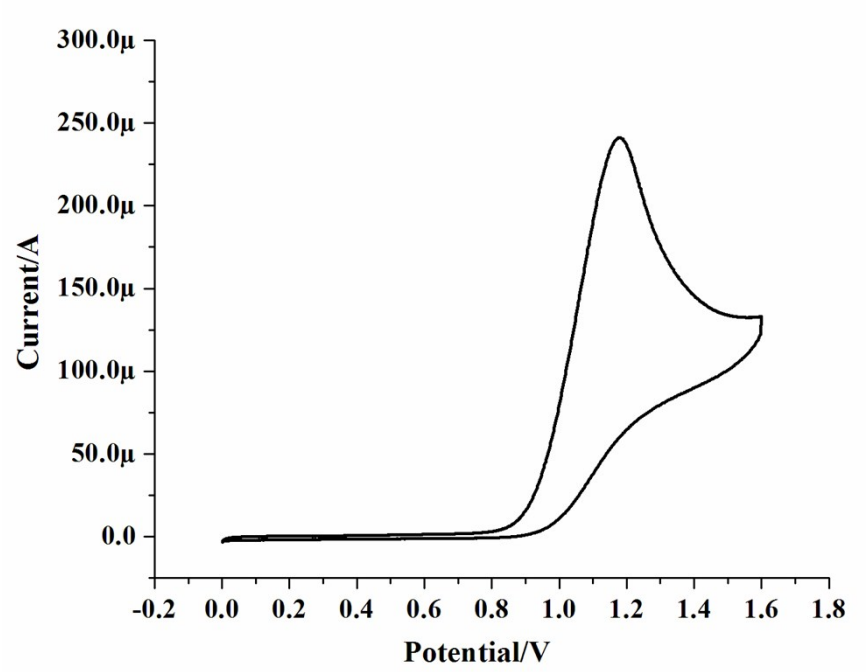

Figure S28: Cyclic voltammogram of NO in methanol solvent. Working electrode, Glassy-carbon; Reference electrode, Ag/AgCl; TBAP supporting electrolyte; scan rate 50 mV/s.